Ruthenium dendrimers against acute promyelocytic leukemia. *In vitro* studies on HL-60 cells

Sylwia Michlewska*,[1,2], Maksim Ionov**,[2], Marta Maroto-Díaz[3,4], Aleksandra Szwed[2], Aliaksei Ihnatsyeu-Kachan[6,7], Viktar Abashkin[8], Volha Dzmitruk[8], Aneta Rogalska[9], Marta Denel[7], Magdalena Gapinska[1], Dzmitry Shcharbin[8], Rafael Gomez Ramirez[3,4,5], Francisco Javier de la Mata[3,4,5] & Maria Bryszewska[2]

[1]Laboratory of Microscopic Imaging & Specialized Biological Techniques, Faculty of Biology & Environmental Protection, University of Lodz, Banacha12/16, Lodz 90–237, Poland
[2]Department of General Biophysics, Faculty of Biology & Environmental Protection, University of Lodz, Pomorska 141/143, Lodz 90–236, Poland
[3]Networking Research Center on Bioengineering, Biomaterials & Nanomedicine (CIBER-BBN), Spain
[4]Departamento Quımica Orgánica y Quımica Inorganica, Universidad de Alcalá, Spain. Instituto de Investigación Quımica "Andrés M. del Rıo" (IQAR), UAH, Spain
[5]Instituto Ramon y Cajal de Investigación Sanitaria, IRYCIS, Spain
[6]Center for Theragnosis, Biomedical Research Institute, Korea Institute of Science & Technology (KIST), Seoul 02792, Korea
[7]Division of Bio-Medical Science & Technology, KIST School, Korea University of Science & Technology (UST), Seoul 02792, Korea
[8]Institute of Biophysics & Cell Engineering of NASB, Akademicheskaja 27, Minsk 220072, Belarus
[9]Department of Medical Biophysics, Faculty of Biology & Protection, University of Lodz, Pomorska 141/143, Lodz 90–236, Poland
*Author for correspondence: sylwia.michlewska@biol.uni.lodz.pl
* **Author for correspondence: maksim.ionov@biol.uni.lodz.pl

Coordination of ruthenium arene fragments on carbosilane dendrimers' surface greatly increases their antitumor properties. Newly synthetized ruthenium dendrimers are water-soluble, monodisperse and stable. Since carbosilane dendrimers are good carriers of drugs and genes, the presence of ruthenium in their structure makes them promising candidates for new drug delivery systems with improved antitumor potential. Carbosilane ruthenium dendrimers are more toxic to cancer cells than normal cells. Results of several *in vitro* studies applied here indicate that carbosilane ruthenium dendrimers induce apoptosis in promyelocytic leukemia HL-60 cells.

Graphical abstract:

In adults (age 15–99), stomach, colorectal, liver, lung, breast, cervix, ovarian, prostate cancer and leukemia are the most common neoplasms [1,2] among children and adolescents, the last has the highest incidence. One of the most difficult problems is to develop an effective and safe drug, considering that the administration of the current pharmaceuticals carry high risks for the patient. The main reason for this is the poor selectivity of the anticancer drugs used, some of which have unwelcome side effects on the body [2].

Among the different types of cell death induced by chemotherapy, the phenomena of apoptosis and necroptosis – programmed cell death – have attracted considerable attention [3]. During apoptosis, typical morphological changes – such as chromatin condensation and marginalization, and shrinking of the nucleus – occur [4,5] and the nucleus becomes fragmented, the cytoplasm becomes dense and the structure of other organelles changes. Ultimately, apoptotic bodies are formed and removed by the phagocytic cells, avoiding any inflammatory process. Two activated pathways can be involved depending on the cell type and the inducing factor. The extrinsic receptor pathway associated with the cell membrane receptors, such as the protein receptor family of tumor necrosis factor and their ligands, is among others. The intrinsic pathway involving mitochondria is activated by an increased

newlands
press

concentration of reactive oxygen species (ROS) and calcium ions in the cytoplasm, oxidative stress, DNA damage and disorders in electrolyte transport [5]. There are other pathways, one in which perforin and granzyme B (pseudoreceptor) are involved, and another involving the endoplasmic reticulum (reticular-induced stress). Consequently, regardless of the agent causing apoptosis, a caspase cascade is activated which results in cell death without an inflammatory reaction.

Tumor cells can avoid activating apoptosis by different pathways [5,6]. Absence, silencing or deactivation of the apoptotic protease activating factor 1 (Apaf-1) in leukemia, glioblastoma, cervical and ovarian cancer cells lead to resistance against many anticancer drugs. This is related with the importance of this cytosol protein in the activation of cytochrome C-dependent apoptotic signaling [7,8]. Multidrug resistance (MDR) is multifactorial and may be mediated by overexpression of anti-apoptotic proteins, such as Bcl-2, Bcl-xL or Mcl-1 or p53, FADD, Bax or Fas mutations [9,10]. Another result of cancer treatment seems to be programmed necrosis, in particularly necroptosis, a process associated by linking the tumor necrosis factor receptors with their ligands, similar to the extrinsic apoptosis pathway. ATP and glucose levels determine whether cells by apoptosis or necroptosis [11,12]. Necroptosis requires active disintegration of mitochondrial, lysosomal and plasma membranes; unlike apoptosis, necroptosis does not need caspase activation [5].

Despite the involvement of new effective drugs to treat cancers, the clinical effects are still far from satisfactory. It can be explained by limited ways of transporting of therapeutic compounds directly to the tumors. This triggers side effects, causing high mortality. For that reason, it is highly important to develop new carries that can deliver the drug substances and reduce their toxicity for healthy tissues and organs [13]. Nanoparticles, such as nanotubes, liposomes or dendrimers have certain advantages over conventional chemotherapeutics because they can be synthesized to have better properties or behave in more specific ways [14,19,20]; properties include selectivity, size, shape and biocompatibility.

In this approach, dendrimers can be useful due to their being highly branched macromolecules of low polydispersity, providing encouraging opportunities for the design of novel drug-carriers. For example, terminal groups conjugated on the surface of these systems generally determine the properties and their application [17].

Our research group works with carbosilane dendrimers. The main features of this scaffold are its lipophilic skeleton (more hydrophilic like polyamidoamine [PAMAM] or polypropylenimine [PPI] in contrast with other types of dendrimers), its chemical inertness and chemical stability. To make them water-soluble, the surface is modified with cationic moieties, thus making them suitable for different biomedical applications since this facilitates their interaction with the surface of cell membranes of an anionic nature [14,15,18–21]. The antitumoral properties of some dendrimers based on 3-diaminobenzidine (DAB), polypropylenimine or carbosilane scaffolds have been enhanced by conjugation on their surface with different metal complexes based on gold, silver, platinum or ruthenium [13–18,26]. Among them, ruthenium-based complexes have now acquired a certain prominence. Ru (III) complexes are reduced to the more reactive Ru (II) form at lower pH and in a tumor-reducing environment [27,28]. Ruthenium derivatives probably use transferrin, to accumulate in tumors, due to their similarities with iron, leading to them being less toxic complexes than their metallic analogs [29–31].

We investigated newly synthetized carbosilane dendrimers with attached ruthenium molecules (carbosilane ruthenium dendrimers [CRD]) as potential anticancer agents. Possible mechanisms of CRD antitumor activities have been analyzed. The results indicate that ruthenium dendrimers with imino-pyridine endgroups induce apoptosis in promyelocytic leukemia cells of the HL-60 line (Figure 1).

Materials & methods

Ruthenium-terminated carbosilane dendrimers (CRD)

Two generations of ruthenium-terminated carbosilane dendrimers with imine(o)-pyridine endgroups have been analyzed. The dendrimer structures and molecular weight are given in Figure 2. To obtain these compounds to a solution of G_n-[NH$_2$]$_m$ in THF, the corresponding aldehyde, 2-pyridinecarboxaldehyde was added. The mixture was stirred under inert atmosphere at room temperature in the presence of anhydrous MgSO$_4$ or 24 h. Subsequently, the solvent was evaporated to give an oil that was purified by size exclusion chromatography. Once the dendritic ligands precursors were obtained, these were dissolved in dry ethanol and then the dimer [Ru(η^6-*p*-cymene) Cl$_2$]$_2$ was added slowly to that solution. The solution was stirred overnight at room temperature; after which, the solvent was evaporated under reduced pressure, affording compounds **CRD 13** and **CRD 27** in moderate yields. The main characteristics and detailed steps of the synthesis of dendrimers have been described elsewhere [26].
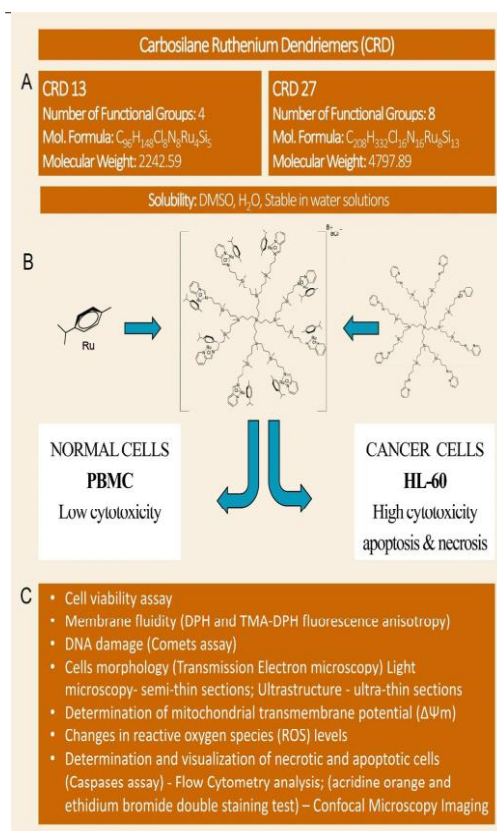
Figure 1. Schematic drawing of the manuscript. (A) Ruthenium dendrimers characterization. **(B)** Effect of dendrimers on PBMC and HL-60 cells. **(C)** *In vitro* techniques used in this study. PBMC: Peripheral blood mononuclear cell.
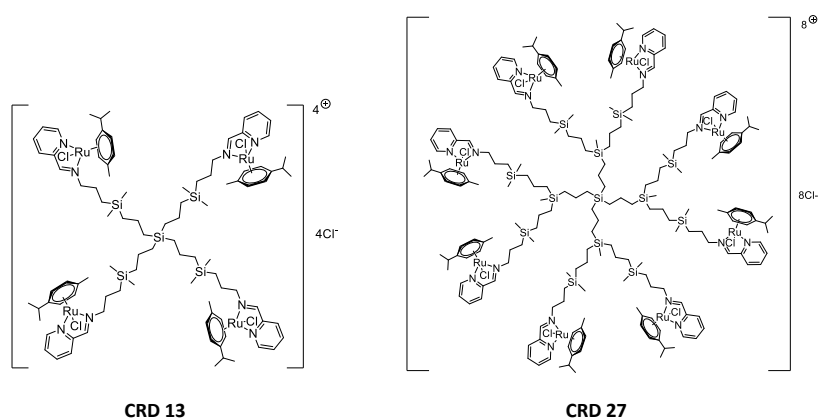

Figure 2. Molecular structure and molecular weight of the ruthenium-terminated carbosilane dendrimers of the first and second generations with imine-pyridine endgroups CRD 13 and CRD 27.

Cell viability

Peripheral blood mononuclear cells

Peripheral blood mononuclear cells (PBMCs) were obtained from healthy donors from the Regional Blood Center in Lodz (Poland). After isolation (Histopaque 1077, Sigma), cells were resuspended in RPMI-1640 (Gibco) with heat-inactivated 10% FBS (HyClone) in the presence of antibiotics (1%). The cells were maintained in plastic tissue culture flasks (Falcon) and kept at 37°C in a humidified atmosphere containing 5% CO_2/95% O_2.

HL-60 cells

HL-60 cell line (human acute leukemia) was purchased from ATCC, UK. Cells (1×10^4 per well) were grown as stated above. The cytotoxicity of dendrimers was assessed by the Alamar Blue assay. After 72 h treatment with dendrimers, PBMC and HL-60 cell viability was calculated from the formula:

$$\% \text{ viability} = (A/A_c) \times 100\%,$$

where A is the absorbance of the sample, and A_c is the absorbance of control cells.

l,6-Diphenyl-l,3,5-hexatriene & 1-(4-(trimethylamino)phenyl)-6-phenylhexa-1,3,5-triene fluorescence anisotropy

To estimate the nature of the interaction between ruthenium dendrimers and cell membranes, the technique of l,6-diphenyl-l,3,5-hexatriene (DPH) and 1-(4-(trimethylamino)phenyl)-6-phenylhexa-1,3,5-triene (TMA-DPH) fluorescence anisotropy was used, with erythrocyte membranes taken as a model. Erythrocytes were hemolysed in cold (4°C) hypotonic 10 mM Na-phosphate buffer, pH 7.4. In order to separate the membranes from hemoglobin they were washed 4–6 times with Na-phosphate buffer. The concentration of membrane protein was calculated using Lowry method [31]. After isolation the membranes were kept frozen for 14 days.

To analyze changes in membrane fluidity induced by adding the dendrimers to the membrane solution, we used fluorescence anisotropy of DPH and TMA-DPH probes. DPH, a nonpolar molecule, enters the hydrophobic region of the lipid membrane, whereas TMA-DPH is anchored near the hydrophilic part of the lipid bilayer due to its positively charged amino groups. Fluorescence anisotropy was measured in rising concentrations of **CRD 13** and **CRD 27** using Perkin–Elmer spectrofluorimeter LS-50B. For the DPH probe, the excitation and emission wavelengths were 348 and 426 nm, respectively; for TMA-DPH, 358 and 428 nm, respectively.

The slit-width of the excitation monochromator was 6 nm and that of the emission monochromator was 8 nm for both probes. Readings were taken at 37°C. Erythrocyte membranes were dissolved in phosphate-buffered saline (PBS), pH 7.4. The concentration of each fluorescent probe was 1 μmol/l. After their addition, the samples were incubated for 10 min. Dendrimers were dissolved in water, and added to the sample to reach the required concentrations. Fluorescence anisotropy values (r) were calculated using Perkin–Elmer software from Jablonski's equation:

$$r = (I_{VV} - GI_{VH}) / (I_{VV} + 2GI_{VH})$$

I_{VV} - vertical fluorescence intensity, I_{VH} - horizontal fluorescence intensity. $G = I_{HV}/I_{HH}$ - grating correction factor that corrects the monochromator polarizing effects.

Comet assay

The comet assay was used under alkaline conditions following the procedure described in [29]. The cells were suspended in 0.75% low melting-point agarose in PBS (pH 7.4); next, the cells at the concentration 5×10^{-2} ml were applied on slides, earlier coated with 1% normal agarose. After this the slides were incubated at 4°C for 1 h in a lysing buffer (2.5 M NaCl, 100 mM EDTA, 1% Triton X-100, 10% DMSO and 10 mM Tris), pH 10. Subsequently, the slides were subjected to electrophoresis in buffer (300 mM NaOH, 1 mM EDTA, pH > 13) for 40 min. Electrophoresis was carried out at 0.73 V/cm, 300 mA for 30 min. DNA was stained with DAPI (4 μg/ml) in the dark, and 50 randomly selected cells were assessed with Nikon E200 (Japan) equipped with a filter UV and Cohu 4910 video camera (Cohu, Inc., CA, USA) and Lucia–Comet v. 4.51 (Laboratory Imaging, Prague, Czech Republic) analysis system. The percentage of DNA in comet tails was measured.

Transmission electron microscopy

Transmission electron microscopy (TEM) analysis of the cancer cells HL-60 was used to analyze ultrastructural changes. The cells were treated with 2.5 μmol/l **CRD 13** or 5 μmol/l **CRD 27** before being incubated for 24 h. After incubation, cells were centrifuged 10 min/1500 r.p.m. and washed twice with PBS. They were fixed with 2.5% glutaraldehyde in 0.1 M PBS (pH 7.2) for 2 h before being dispersed in 1.5% agarose and rinsed three-times with the same buffer. The cells were postfixed in 1% osmium tetraoxide for 2 h at 4°C, and dehydrated in ethanol and propylene oxide before being embedded in Epon–Spur's resin mixture. Semithin sections were stained with 1% toluidine blue to examine cell morphology by light microscopy with a Nikon Eclipse 50i, using Coolview software. Ultrathin sections (70–80 nm) were putted on formvar-coated nickel grids (300 mesh) and stained with uranyl acetate and lead citrate [30]. Ultrastructure of the cells was evaluated with the transmission electron microscope JEM 1010 (JEOL, Japan) at 80 kV.

Determination of ROS levels

HL-60 cells were treated with dendrimers at from 0.5 to 5 μmol/L. After treatment, cells suspensions were incubated in 2.5 μmol/L H_2DCF-DA PBS-based solution for 20 min under growth conditions. Fluorescence measurements were subsequently carried out using a BioTek Synergy HTX microplate spectrophotometer at λ_{ex} = 485 and λ_{em} = 528 nm. The ROS level was calculated relatively to the control. The results were obtained from 3 independent experiments and are given as mean ± standard deviation (SD).

Mitochondrial transmembrane potential

To measure mitochondrial transmembrane potential HL-60 cells were incubated for 0.5, 3, 24, 48 and 72 h in the presence of dendrimers from 0.5 to 5 μmol/l. A 5 μmol/l of fluorescent dye C-1 (5,5′,6,6′-tetrachloro-1,1′,3,3′ tetraethylbenz-imidazolcarbocyanide iodide) was added to each well [28]. Measurements were taken after 20 min incubation in the dark. The filters used were suitable for fluorescence monomers (l_{ex} = 485 nm, l_{em} = 538 nm) and
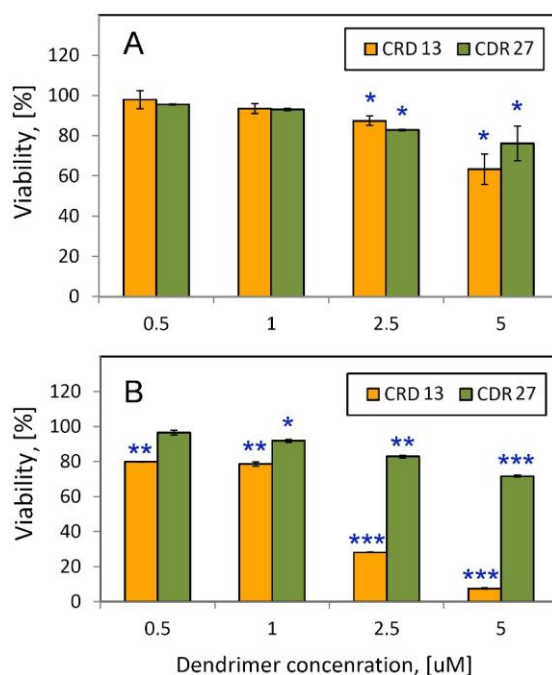

Figure 3.   Effect of carbosilane ruthenium dendrimers on the viability of: (A) normal PBMC cells and **(B)** HL-60 cancer cells after 72-h incubation. The values are the mean ± SD of n > 6. *Statistically significant differences in comparison to the control cells (*p < 0.05, **p < 0.01, ***p < 0.001). PBMC: Peripheral blood mononuclear cell.

fluorescence dimers (l_{ex} = 530 nm, l_{em} = 590 nm). Measurements (mitochondrial membrane potential [m]) were made using a Fluoroscan Ascent FL microplate reader. The fluorescence factor was calculated:

$$m = \frac{F_D}{F_M}$$

where m is the mitochondrial potential directly proportional to the fluorescence factor, F_D the dimer fluorescence and F_M the monomer fluorescence. The results have been expressed as % of the control (100%). Experiments were repeated three-times and the results averaged.

Determination of necrotic & apoptotic cells by the caspase test

To estimate the influence of ruthenium dendrimers on the changes in the number of apoptotic and necrotic cells, we used the caspase test. Exponentially growing HL-60 cells (3–5 × 10^5 cells/ml) were treated with the apoptosisinducing agent, staurosporine, at 0.5 μmol/l (Sigma), propidium iodide (PI)-positive control ETOH or CRD dendrimers. In cells collected at 24 and 48 h after incubation, detection of activated caspases by their fluorescently labeled inhibitors (FLICA) was combined with plasma membrane permeability assessment (PI). The cells were stained with FAM-VAD-FMK (pan caspase marker; fluorescently labeled inhibitors) for 2 h and PI. Samples were analyzed by flow cytometry. Triplicate cultures were measured per treatment.

Determination of necrotic & apoptotic cells by the acridine orange and ethidium bromide test

To distinguish apoptotic and necrotic cells, the double staining test with acridine orange (AO) and ethidium bromide (EB) – DNA-binding fluorescent dyes – was used [32]. AO stains the nuclei green; whereas, EB stains cells with damaged membranes in red.

To assess the state of cells, the following criteria were used: normal green nucleus - viable cells, green nucleus with condensed or fragmented chromatin - early apoptotic cells, condensed or fragmented orange/red chromatin -late apoptotic cells, red nucleus - necrotic cells.

The cells were grown at 1 × 10^5 cells per well on 24-well plates in RPMI medium. They were treated with dendrimers (**CRD 13**: 2.5 and 5 μmol/l and **CRD 27**: 5 and 7.5 μmol/l) for 24 h. The AO/EB mixture was added to each plate at 2 μg/ml and the cells examined by confocal microscopy (Leica TCS SP8).

Results Viability

The cytotoxic activity of the new carbosilane metallodendrimers based on arene ruthenium (II) complexes **CRD 13** and **CRD 27** against peripheral blood mononuclear normal cell line (PBMC) and promyelocytic leukemia cancer cell line (HL-60) was evaluated using the Alamar Blue assay.

The results are summarized in Figure 3. The results show that CRDs are more cytotoxic against cancer cells. The effect of dendrimers on PBMC and HL-60 cell viability was estimated by the incubation of cells with **CRD 13** or **CRD 27** for 72 h. The data showed weak changes in viability of PBMC cells in the presence of both dendrimers

Table 1. Inhibitor concentrations (IC$_{50}$, μM) resulting in 50% dendrimers-mediated reduction of HL-60 cell viability.			
	IC$_{50}$, HL-60		
Dendrimer	24 h	48 h	72 h
CRD 13	11.6 ± 1.6	3.70 ± 3.9	2.32 ± 0.4
CRD 27	12.9 ± 2.1	12.29 ± 3.9	11.36 ± 2.3

Incubation time 24, 48 and 72 h.
Results are mean ± SD, n = 6.
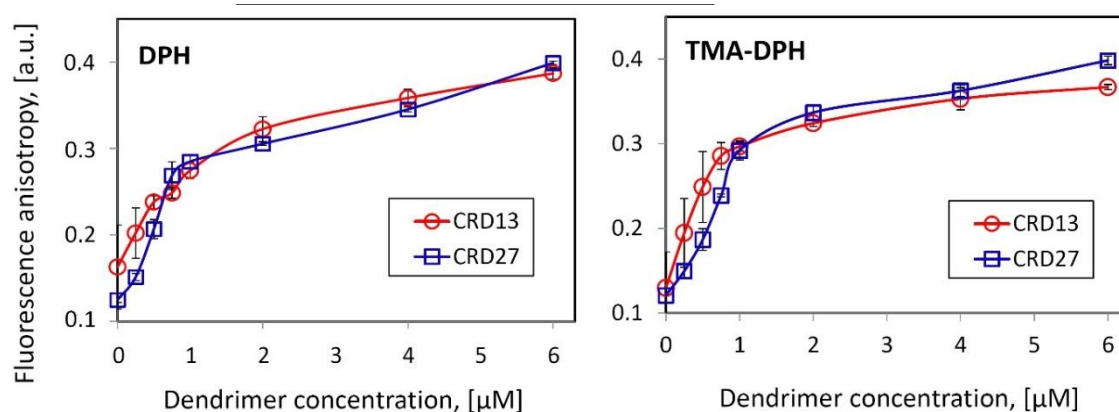
CRD: Carbosilane ruthenium dendrimer.

Figure 4. Changes in fluorescence anisotropy of l,6-diphenyl-l,3,5-hexatriene (left panel) and 1-(4-(trimethylamino)phenyl)-6-phenylhexa-1,3,5-triene (right panel) of erythrocyte membranes treated by ruthenium dendrimers. PBS buffer, pH 7.4, 37°C. The values are the mean ± SD of three independent experiments. PBS: Phosphate-buffered saline.

at from 0.5 to 5 µmol/l. In contrast, the viability of cancer HL-60 cells was significantly decreased in the presence of **CRD 13** (Figure 3).

CRD 13 is more cytotoxic than **CRD 27**. While **CRD 27** (5 µmol/l) reduced viability of HL-60 cells up to 71.6 ± 0.5 %, **CRD 13** at 2.5 and 5 µmol/l reduced viability to 28.1 ± 0.14% and 7.47 ± 0.32%, respectively. The IC_{50} values of **CRD 13** and **CRD 27** for HL-60 cell line are summarized in Table 1.

Fluorescence anisotropy measurements

To discover how ruthenium dendrimers influence cancer cells, we applied a series of experiments using different techniques. First, the ability of dendrimers to influence the cell membrane was determined. Red blood cell membrane fluidity changes induced by incorporation of the investigated dendrimers were measured by DPH and TMA-DPH fluorescence anisotropy. Increasing concentrations of dendrimers in the membrane suspension changed the anisotropy of samples, indicating changes in membrane fluidity. For both dendrimers from 0.5 to 6 µmol/l, there was a significantly increasing dose-dependent anisotropy of DPH and TMA-DPH (Figure 4). An increase in DPH and TMA-DPH fluorescence anisotropy was noted, which may indicate that **CRD 13** and **CRD 27** interact with both hydrophobic and hydrophilic regions of the membrane. Changes in fluorescence anisotropy were similar for **CRD 13** and **CRD 27**.

Comet assay

The Comet assay was used to assess whether dendrimers can induce DNA damage in single cells by determining the percentage of degraded DNA. Due to the different activity of the dendrimers, the concentration range from 2.5 to 5 µmol/l for **CRD 13** and 5 to 7.5 µmol/l for **CRD 27** were chosen. Figure 5 shows the representative comets of the alkaline version for control and dendrimer-treated HL-60 cells after 24 h incubation. Comets of the control cells had almost symmetrical shape and no tails; whereas, comets from the cells treated with **CRD 13** or **CRD 27** had long tails. Moreover, the images of dendrimer-loaded cells clearly show the typical comets of apoptotic cells. The mean value (%) of DNA damage depended on the dendrimer type. The results clearly demonstrate that cells treated with dendrimer **CRD 13** had a mean level of basal DNA damage for both concentrations compared with cells treated with dendrimer **CRD 27**. The highest level of DNA in the comet tail (39.15 ± 1.14 %) in the same cell line was obtained after incubation with **CRD 13** at 2.5 µmol/l (the lower of the concentrations).
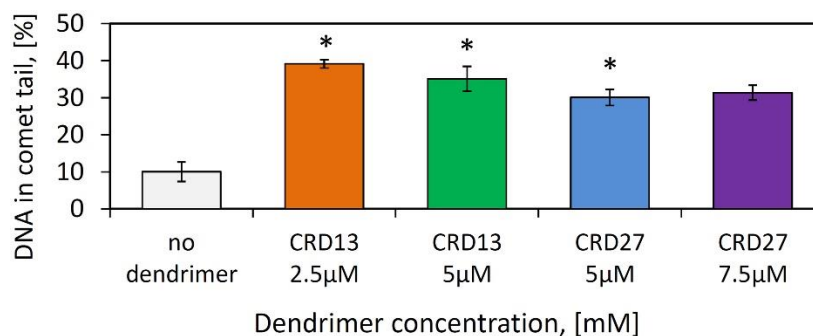
Figure 5. DNA [%] in comet tail of the control in HL-60 cells and cells-treated different concentrations of CRD 13 (2.5 and 5 μmol/l) and CRD 27 (5 and 7.5 μmol/l) dendrimers. The number of cells analyzed in each treatment was 50. The values are the mean ± SD of three independent experiments. *$p < 0.05$ statistically significant differences in comparison to control cells.
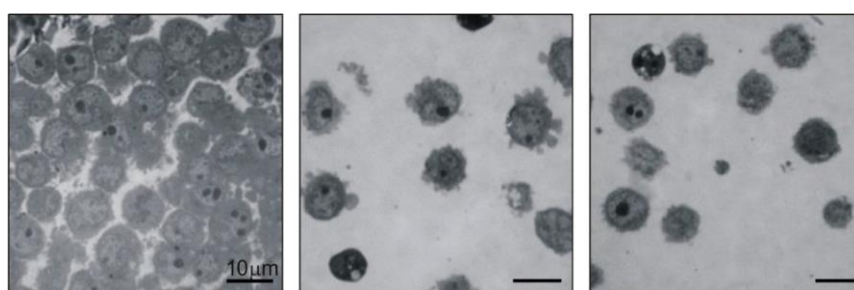

Figure 6.   Light microscopy of semi-thin sections of HL-60 cells: (A) naked cells; **(B)** cells treated with CRD 13 in a concentration of 2.5 μmol/l; **(C)** cells treated with CRD 27 in a concentration of 5 μmol/l. Scale bar = 10 μμm. CRD: Carbosilane ruthenium dendrimer.

Under these conditions, the differences between the untreated (control) cells and those exposed to dendrimers at all concentrations were statistically significant (Figure 5).

Transmission electron microscopy

Light microscopy: semi-thin sections

Figure 6 shows several morphological changes of HL-60 cells affected by **CRD13** at concentration of 2.5 μmol/l and **CRD27** concentration of 5 μmol/l. Characteristic features indicating apoptosis such as compaction of chromatin in dense clots, condensation of cytoplasm, cytoplasmic vacuolization and appearance of numerous vesicular structures can be seen (Figure 6B,C). Chromatin condensation can also be associated with necrosis induced by dendrimers (Figure 6B,C). Light microscopy confirmed the data from the analysis of electron microscopy images described below.

Ultrastructure: ultra-thin sections

TEM was used to examine ultrastructural changes in HL-60 cells following **CDR 13** at concentration of 2.5 μmol/l and **CDR 27** at concentration of 5 μmol/l treatment. Figure 7 shows that control untreated cells had a typical ultrastructure, including numerous microvilli on the surface, evenly distributed chromatin and numerous normal shape mitochondria in the cytoplasm (Figure 7A). In contrast, the ultrastructure of HL-60 cells treated with **CRD 13** demonstrated typical morphological features of early apoptosis, including shape changes and shrinking of cells, denser cytoplasm, chromatin marginalization and condensation (Figure 7D,E). Multi-vesicular and lamellar bodies were seen in these cells. Mitochondria were swollen and their membranes damaged (Figure 7F), and fragmentation of plasmolemma was present (Figure 7G). After addition of **CRD 27**, the shape of the HL-60 cells was significantly modified. Multivesicular and lamellar bodies were clearly visible (Figure 7H). The cell fragment in Figure 7I shows how dendrimers can be internalized by cells. The endocytic
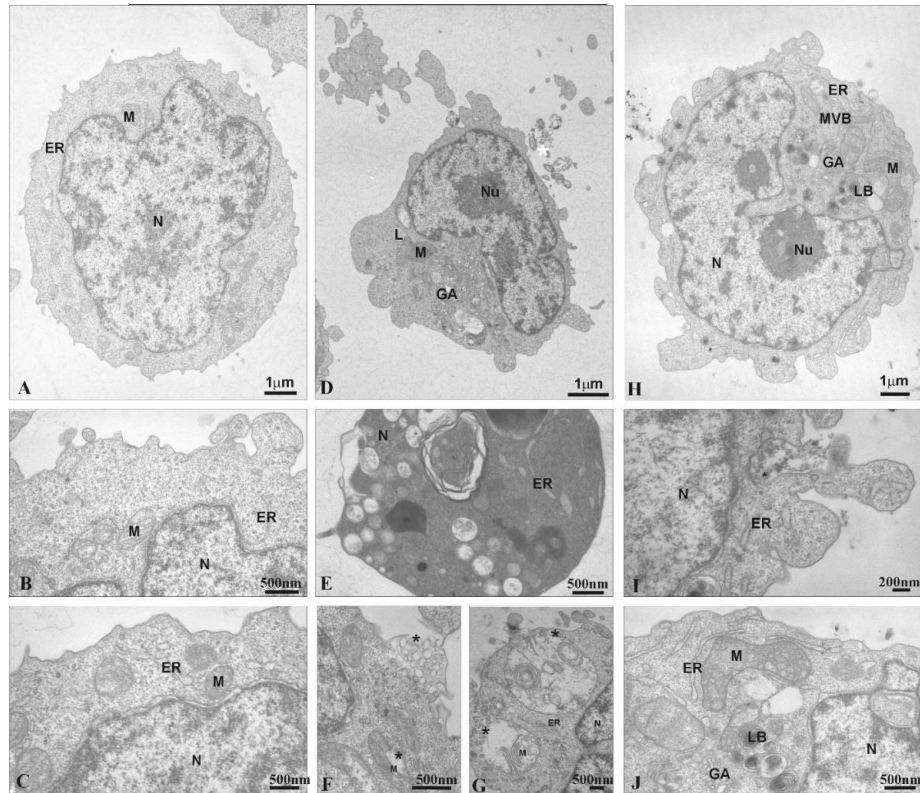
Figure 7.   Ultrastructural changes of HL-60 cells **(A–C)**; HL-60 cells treated with **CRD 13**, 2.5 µmol/l **(D–G)** and **CRD 27**, 5 µmol/l **(H–J)**. *: vesicle contained CRD dendrimers. ER: Endoplasmicreticulum; GA: Golgi apparatus; L: Lipids; LB: Lamellar body; M: Mitochondria; MVB: Multivesicular body: N: Nucleus; Nu: Nucleolus.
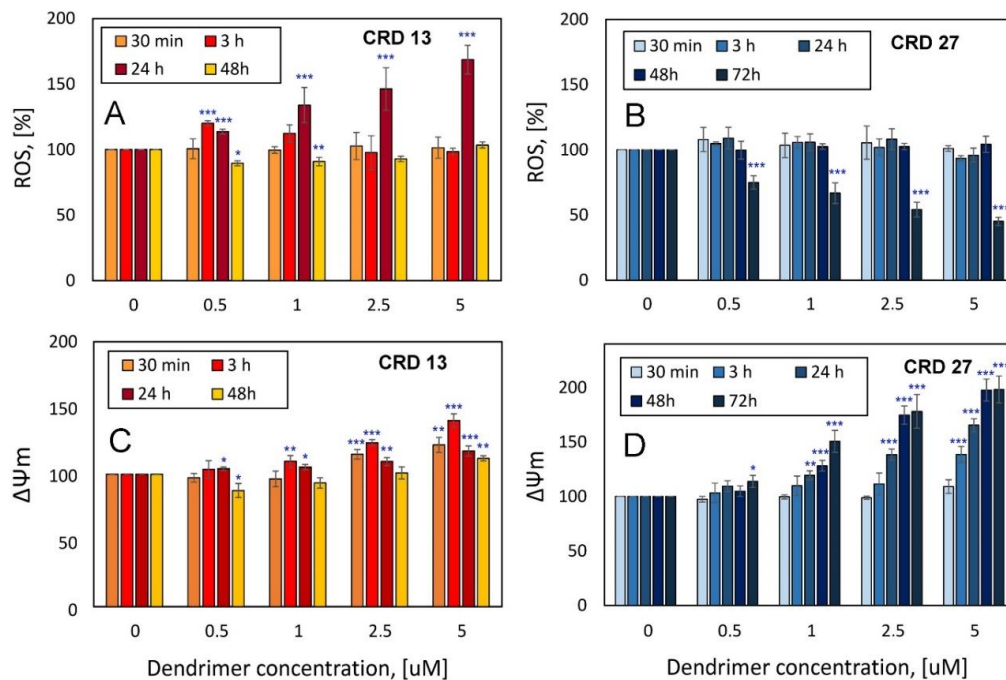

Figure 8.   The changes of the ROS levels **(A & B)** and m **(C & D)** in HL-60 cells under influence of ruthenium dendrimers, **CRD 13** (left panels), **CRD 27** (right panels). The values are the mean ± SD of six independent experiments (*p < 0.05, **p < 0.01, ***p < 0.001). *Statistically significant differences compared control cells. ΔΨm: Mitochondrial membrane potential; ROS: Reactive oxygen species.

vesicle (star) containing dendrimers move into the cell. This image confirms the assumption of a possible mechanism of dendrimer internalization in the cells. CRDs can probably be taken up by endocytosis.

ROS & ΔΨm

After analyzing the TEM images, we supposed that morphological changes of HL-60 cells induced by ruthenium dendrimers are due to an increased level of ROS or mitochondrial potential modifications. The data indicate that both of these parameters are influenced by CRDs. To evaluate changes in the level of ROS a fluorescent probe H_2DCFDA was used.

After 48 h incubation of HL-60 cells with **CRD 27,** there were no significant changes in the level of ROS compared with the control. After 72 h ROS levels decreased for all concentrations, with a minimum at $45.1 \pm 3.1\%$ for 5 µmol/l versus control (Figure 8B). Due to the higher cytotoxicity of **CRD13** compared with **CRD 27**, the ROS level in the cells treated with **CRD 13** was measured at 48 h. In the presence of **CRD 13,** the levels of ROS started increasing after 3 h incubation reaching maximal values at 2.5 and 5 µmol/l, up to $146.2 \pm 16.2\%$ and $168.6 \pm 10.9\%$, respectively, after 24 h incubation. Following 48 h incubation, the level of ROS decreased to control values (Figure 8A).

Changes in m of HL-60 cells were estimated by JC-1 probe fluorescence. Cells were treated with **CRD 13** and **CRD 27** dendrimers at from 0.5 to 5 µmol/l for 0.5, 3, 24, 48 and 72 h. Both dendrimers changed m, causing the highest hyperpolarization at 5 µmol/l and after an incubation time of 3 h for **CRD 13** and 48–72 h for **CRD 27**. The maximal mitochondrial hyperpolarization was shown for **CRD 27** for 72 h incubation, where the potential increased to $198.2 \pm 12.3\%$ versus control.
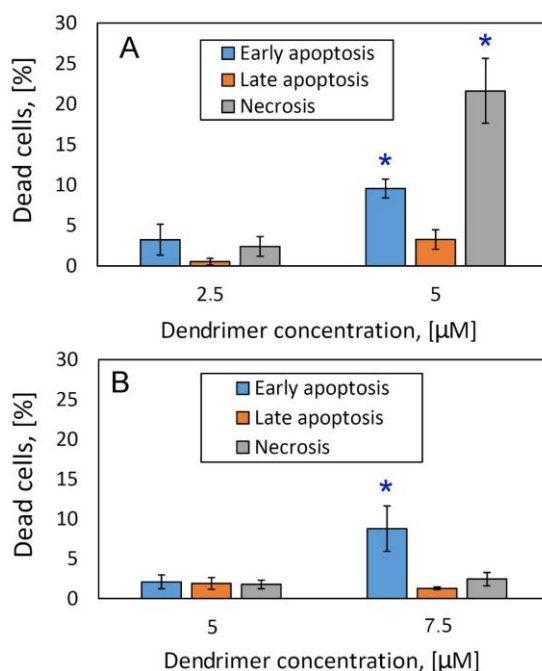

Figure 9.   Percentage of HL-60 cells after 24 h incubation with ruthenium dendrimers. (A) CRD 13 at the concentration from 2.5 to 5 µmol/l; **(B) CRD 27** the concentration range from 5 to 7.5 µmol/l.
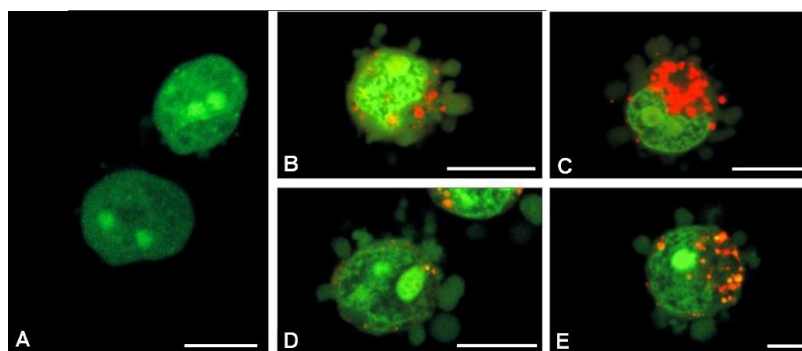
Figure 10. Confocal microscopy images of HL-60 cells after 24 h treatment with carbosilane ruthenium dendrimer. (A) control, **(B) CRD 13** 2.5 μmol/l, **(C) CRD 13** 5 μmol/l, **(D) CRD 27** 5 μmol/l, **(E) CRD 27** 7.5 μmol/l. Cells were stained with AO/EB. Scale bar = 5 μm.
AO/EB: Acridine orange/ethidium bromide dual staining.

Caspases assay: flow cytometry analysis

Using previously described methods, ruthenium dendrimers can be shown to induce apoptosis of HL-60 cells. Using the caspase assay, we measured the percentage of apoptotic cells treated with **CRD 13** and **CRD 27**. After 24 h culturing with CRDs, caspase activity increased with increasing dendrimer concentration. After treatment with 2.5 μmol/l **CRD 13** or 5 μmol/l **CRD 27**, small levels of early and late apoptotic cells were detected, in other words, early apoptotic cells constituted 3.2 ± 1.9% and 2.1 ± 0.9% of all cells, respectively, whereas late apoptotic cells were 0.5 ± 0.4% and 1.9 ± 0.7%, respectively. There were 2.4 ± 1.2% and 1.8 ± 0.5% necrotic cells, respectively, under the same conditions. **CRD 27** at 7.5 μmol/l increased the number of early apoptotic cells to 8.8 ± 2.9%, whereas 5 μmol/l **CRD 13** significantly increased the necrotic cells to 21.6 ± 4.0% (Figure 9)

Visualization of apoptosis & necrosis by AO/EB double staining

The AO/EB double staining technique showed the ability of ruthenium dendrimers to induce apoptosis, visualized by confocal microscopy was applied. As it is shown in Figure 9, flow cytometry results correlate with those from confocal microscopy. The 24-hour treatment of HL-60 cells with **CRD 13** 2.5 μmol/l or **CRD 27** 5 μmol/l led to the appearance of early apoptotic cells. At the presence of both dendrimers at higher concentrations (5 μmol/l **CRD 13** or 7.5 μmol/l **CRD 27**) respectively, mainly late apoptotic cells were present in the HL-60 cells suspension (Figure 10).

Discussion

Due to their universality, dendrimers may be the most promising among currently known types of nanoparticles for use in several fields of science, especially medicine. Dendrimers have extraordinary potential against neurodegenerative diseases [37] and cancers [14], as drug and gene-carriers [38].

Carbosilane ruthenium-terminated dendrimers were significantly more cytotoxic against HL-60 cancer cells compared with PBMC normal cells. Similar effects, in other words, where carbosilane dendrimers were not cytotoxic against PBMC cells, have previously been reported [38]. Moreover, using carbosilane dendrimers with various terminal groups against mHippo-18 cells did not influence the number of living cells [37]. However, when the CRD dendrimers were incubated with HL-60 cells, their viability decreased. The first generation of CRD dendrimer (**CRD 13**) was more cytotoxic than the second generation dendrimer (**CRD 27**).

Significant effects of ruthenium-containing complexes [39,40] and ruthenium dendrimers have been reported several tumor cell lines [14,26]. CRD dendrimers have a number (appropriate to generation) of positive surface charges [14], which enables them to form electrostatic complexes with negatively charged drugs and nucleic acids, making them potential transporters of these substances [14,37].

We used HL-60 cells to determine the mechanism of action of ruthenium dendrimers. Cationic dendrimers can interact with negatively charged cell membranes, which allows them to cross the membrane barrier. However, this can create microholes in the membrane and consequently lead to cell death, making dendrimers cytotoxic [41]. To determine the interaction of CRDs with cell membranes, we used the fluorescence of DPH and DMA-DPH probes internalized into red blood cell membrane. CRD dendrimers interact with both hydrophobic and hydrophilic regions of membrane, altering lipid order and membrane fluidity. Similar interactions of other dendrimers have been described [42]. The hemolytic effect of CRD has been detected [14].

Ruthenium in dendrimers is a metal with antitumor properties [39,43]. Our cytotoxicity studies confirm this, showing the ability of CRDs to reduce HL-60 cells viability. Despite the smaller number of ruthenium molecules in their structure, the first generation (**CRD 13**) was significantly more cytotoxic than the second generation (**CRD 27**). To analyze the difference between effects of our dendrimers, we measured ROS levels and mitochondrial potential changes. Both tests involved dendrimers at from 0.5 to 5 μmol/l, and incubation times were 0.5–72 h for **CRD 27**, but only up to 48 h for **CRD 13** due to its higher cytotoxicity. **CRD 27** did not change ROS levels up to 48 h, but by 72 h there was a sharp decline. The effect of **CRD 13** was different; after 24 h a rapid increase in ROS level occurred, but after a further 24 h, it dropped to the control level. Carbosilane dendrimers did not induce oxidative stress in mHippo-18 cells [37]. However, diruthenium-1 complexes caused a rapid rise of ROS in MCF-7 cancer cells [39]. While **CRD 13** did not change mitochondrial potential, **CRD 27** at high concentrations hyperpolarized mitochondrial membranes of HL-60 up to 198%. Carbosilane dendrimers did not alter mitochondrial potential of mHippo-18 cells [37], whereas treatment of MCF-7 cancer cells with diruthenium-1 led to hyperpolarization [39]. Oxidative stress is most often associated with a decrease in mitochondrial potential, which may indicate the onset of apoptosis [39]. Complexes containing ruthenium molecules induce apoptosis by the intrinsic pathway, connected to mitochondria [39,43]. To clarify the mechanisms of cytotoxicity in HL-60 cells, comet assay showed that DNA damage depended on the type of dendrimer. **CRD 13** generated more DNA damage in HL-60 cells than **CRD 27**. This effect can be explained by the presence of ruthenium, which, like other metals with anticancer properties, can interact with DNA [44]. DNA damage caused by ruthenium complexes was seen for different types of cells [39,40]. Increase in damaged DNA associated with decrease in mitochondrial potential; and a high level of ROS indicates that cells entered the apoptotic pathway [39].

To determine the type of HL-60 cell death after treatment with CRDs, caspases and AO/EB tests were used. Changes in morphology and ultrastructure of HL-60 cells were also analyzed. After 24-h incubation of HL-60 cells with our dendrimers, symptoms of early apoptosis were observed. The caspases test (mediators of apoptosis) showed that the number of apoptotic cells having higher caspase activity increased with the dendrimer concentration. After treatment of HL-60 with **CRD 13** and **CRD 27** at lower concentrations, very small numbers of early and late apoptotic cells were detected, along with a few necrotic cells. At the higher concentration, **CRD 27** increased the number of early apoptotic cells, whereas **CRD 13** led to the appearance of significant numbers of necrotic cells. Both the AO/EB test and the images of the semi-thin sections demonstrate that 24 h treatment of HL-60 cells with **CRD 13** and **CRD 27** led to the appearance of cells with characteristic apoptotic features, in other words, chromatin condensation and fragmentation, as well as apoptotic cellular bubbles (probably apoptotic bodies). Detailed ultrastructural analysis of HL-60 cells treated with **CRD 27** showed relatively gentle alterations and the way dendrimers might be taken up by endocytosis. The mechanism of clathrin-dependent internalization in HL-60 cells was determined for poly(propyleneimnie) glycodendrimers [46]. Similarly, a study on nanodiamonds showed that they can be taken into cells by macropinocytosis and clathrin-mediated endocytosis [45]. In the presence of **CRD 13**, HL-60 suspension caused visible changes in cell structure, a significant proportion of the cells was characterized by distinct chromatin condensation, with changes in mitochondrial shape and appearance of multivesicular and lamellar bodies. These features are characteristic of early apoptosis [5,47]. Similar changes were seen in different types of cancer cells treated with CPT6 [(campthothecin-20 (s)-O-(2-pyrazul-l) acetic ester] [48] and

polyamidoamine/Flag-apoptin [49]. Numerous cells with marked cell membrane fragmentation and mitochondrial membrane discontinuity were also seen after HL-60 cells had been treated with **CRD 13**. Mitochondria were also strongly swollen, with disorganization of their cristae. These changes are characteristic of necrotic cells [5,11,12].

Summarizing, the results obtained showed that CRD can initiate apoptosis in acute promyelocytic leukemia HL-60 cells. Despite the fact that exact apoptosis pathway caused by **CRD**s was not revealed in this study the results show that **CRD** dendrimers, in particular **CRD13**, were effective against cancer HL-60 cells but not for normal cells. Depending on the cells condition, availability of glucose and in particular of ATP in the presence of dendrimers, in some cells apoptotic while in others necroptotic death pathways can be activated.

The **CRD 13** was cytotoxic for cancer but not normal human cell lines, whereas **CRD 27** showed low toxicity against both, probably due to its bigger size. Taking into account the mechanism of **CRD 13** action, this compound can be considered as a potential antitumor agent, thus it is planned to explore **CRD 13** effect when applied together with anticancer drugs or as carriers of these drugs or of nucleic acids.

Future perspective

Our findings suggest that **CRD 13** dendrimer can be considered as a potential antitumor drug; moreover it can be used as a drug carrier for the drug delivery purposes. Thus it is planned to combine the effect of **CRD 13** with the anticancer drugs as well as nucleic acids used in anticancer gene therapy. Such complexes can show more effective therapeutic potential than each agent alone. The new systems can be applied in modern biomedicine.

Summary points

- The present work explores the potential of carbosilane ruthenium dendrimers (CRDs) **CRD13** and **CRD 27** to reduce the proliferation of promyelocytic leukemia cancer cells (HL-60).
- The mechanisms of **CRD**s antitumor effects were characterized by various methods, cell membrane interaction, DNA damage and *in vitro* cell line studies were also performed.
- Despite the smaller number of ruthenium molecules in their structure, the **CRD 13** was significantly more toxic towards HL-60 cells than the **CRD 27** dendrimer.
- Presence of **CRD 13** in HL-60 suspension caused visible changes in cell structure, cells were characterized by distinct chromatin condensation, with changes in mitochondrial shape and appearance of multivesicular and lamellar bodies. These features are characteristic of early apoptosis.
- Results corroborate that **CRD** dendrimers, in particular **CRD13,** were effective against cancer HL-60 cells but not normal cells.
- This work examines a perspective to use **CRD** dendrimers as drugs or promising drug/gene carriers for the therapy of cancer.

Ethical conduct of research

The authors state that they have obtained appropriate institutional review board approval or have followed the principles outlined in the Declaration of Helsinki for all human or animal experimental investigations.

References

1   Allemani C, Weir HK, Carreira H *et al.* Global surveillance of cancer survival 1995–2009: analysis of individual data for 25 676 887 patients from 279 population based registries in 67 countries (CONCORD-2). *Lancet* 385, 977–1010 (2015).

2   Zhang N, Li S, Huab H *et al.* Low density lipoprotein receptor targeted doxorubicin/DNA-gold nanorods as a chemo- and thermo-dual therapy for prostate cancer. *Int. J. Pharm.* 513, 376–386 (2016).

3   Chen D, Yu J, .Zhang L. Necroptosis: an alternative cell death program defending against cancer. *Biochim. Biophys. Acta* 1865, 228–236 (2016).

4   Elmore S. Apoptosis: a review of programmed cell death. *Toxicol. Pathol.* 35, 495–516 (2007).

5   Dasgupta A, Nomura M, Shuck R, Yustein J. Cancer's achilles' heel: apoptosis and necroptosis to the rescue. *Int. J. Mol. Sci.* 18, 23 (2017).

6   Hanahan D, Weinberg RA. Hallmarks of cancer: the next generation. *Cell* 144, 646–674 (2011).

7   Hajra KM, Liu JR. Apoptosome dysfunction in human cancer. *Apoptosis* 9, 691–704 (2004).

8   Fadeel B, Ottosson A, Pervaiz S. Big wheel keeps on turning: apoptosome regulation and its role in chemoresistance. *Cell Death Differ.* 15, 443–452 (2008).

9   Holohan C, Van Schaeybroeck S, Longley DB, Johnston PG. Cancer drug resistance: an evolving paradigm. *Nat. Rev. Cancer* 13, 714–726 (2013).

10   Su Z, Yang Z, Xie L, DeWitt JP, Chen Y. Cancer therapy in the necroptosis era. *Cell Death Differ.* 23, 748–756 (2016).

11   Zhivotovsky B, Orrenius S. Clinical perspectives of cell death: where we are and where to go... *Apoptosis* 14, 333–335 (2009).

12   Galluzzi L, Maiuri MC, Vitale I *et al.* Cell death modalities: classification and pathophysiological implication. *Cell Death Differ.* 14, 1237–1243 (2007).

13   Abbasi E, Aval SF, Akbarzadeh A *et al.* Dendrimers: synthesis, applications, and properties. *Nanoscale Res. Lett.* 9, 247 (2014).

14   Michlewska S, Ionov M, Shcharbin D *et al.* Ruthenium metallodendrimers with anticancer potential in an acute promyelocytic leukemia (HL60) cell line. *Eur. Polm. J.* 87, 39–47 (2017).

15   Matai I, Sachdev A, Gopinath P. Multicomponent 5-fluorouracil loaded PAMAM stabilized-silver nanocomposites synergistically induce apoptosis in human cancer cells. *Biomater. Sci.* 3, 457–68 (2015).

16   Golshan M, Salami-Kalajahi M, Mirshekarpour M, Roghani-Mamaqani H, Mohammadi M. Synthesis and characterization of poly(propylene imine)-dendrimer-grafted gold nanoparticles as nanocarriers of doxorubicin. *Colloids Surf. B Biointerfaces* 55, 257–265. (2017).

17   Khutale GV, Casey A. Synthesis and characterization of a multifunctional gold-doxorubicin nanoparticle system for pH triggered intracellular anticancer drug release. *Eur. J. Phar. Biopharm.* 119, 372–380 (2017).

18   Li YF, Zhang HT, Xin L. Hyaluronic acid-modified polyamidoamine dendrimer G5-entrapped gold nanoparticles delivering METase gene inhibits gastric tumor growth via targeting CD44+ gastric cancer cells. *J. Cancer. Res. Clin. Oncol.* 144, 1463–1473 (2018).

19   Dzmitruk V, Szulc A, Shcharbin D *et al.* Anticancer siRNA cocktails as a novel tool to treat cancer cells. Part (B), Efficiency of pharmacological action. *Int. J. Pharm.* 485, 288–294 (2015).

20   Ionov M, Ihnatsyeu-Kachan A, Michlewska S *et al.* Effect of dendrimers on selected enzymes - evaluation of nano carriers. *Int. J. Pharm.* 499, 247–254 (2016).

21   Pandi P, Jain A, Kommineni N, Ionov M, Bryszewska M, Khan W. Dendrimer as a new potential carrier for topical delivery of siRNA: a comparative study of dendriplex vs. lipoplex for delivery of TNF-α siRNA. *Int. J. Pharm.* 550(1-2), 240–250 (2018).

22   Shcharbin D, Shcharbina N, Milowska K *et al.* Interference of cationic polymeric nanoparticles with clinical chemistry tests-clinical relevance. *Int. J. Pharm.* 473, 599–606 (2014).

23   Klajnert B, Bryszewska M. Dendrimers: properties and applications. *Acta Biochem. Polonica.* 48, 199–208 (2001).

24   Ionov M, Lazniewska J, Dzmitruk V *et al.* Anticancer siRNA cocktails as a novel tool to treat cancer cells. Part (A). Mechanisms of interaction, *Int. J. Pharm.* 485, 261–269 (2015).

25   Kesharwani P, Jain K, Narendra KJ. Dendrimer as nanocarrier for drug delivery. *Progr. Pol. Sci.* 39, 268–307 (2014).

26   Maroto-Dıaz´ M, Elie BT, Gomez-Sal P, P´erez-Serrano J, G´omez R, Contel M, de la Mata FJ. Synthesis and anticancer activity of´ carbosilane metallodendrimers based on arene ruthenium(II) complexes. *Dalton Trans.* 45, 7049–7066 (2016).

27   Pereira FC, Lima AP, Vilanova-Costa CA *et al.* Cytotoxic effects of the compound cistetraammine (oxalato) ruthenium(III) dithionate on K-562 human chronic myelogenous leukemia cells. *Springerplus* 3, 301 (2014).

28   Antonarakis ES, Emadi A. Ruthenium-based chemotherapeutics: are they ready for prime time? *Cancer Chemother. Pharmacol.* 66, 1–9 (2010).

29   Dragutan I, Dragutan V, Demonceau A. Editorial of special issue ruthenium complex: the expanding chemistry of the ruthenium complexes. *Molecules* 20, 17244–17274 (2015).

30   Carter R, Westhorpe A, Romero MJ *et al.* Radiosensitisation of human colorectal cancer cells by ruthenium(II) arene anticancer complexes. *Sci. Rep.* 20596(6), 1–12 (2016).

31   Spreckelmeyer S, Orvig C, Casini A. Cellular transport mechanisms of cytotoxic metallodrugs: an overview beyond cisplatin. *Molecules* 19, 15584–15610 (2014).

32   Salvioli S, Ardizzoni A, Franceschi C, Cossarizza A. JC-1, but not DiOC6(3) or rhodamine 123, is a reliable fluorescent probe to assess delta psi changes in intact cells: implications for studies on mitochondrial functionality during apoptosis. *FEBS Lett.* 411, 77–82 (1997).

33   Singh NP, McCoy MT, Tice RR. A simple technique for quantitation of low levels of DNA damage in individual cells. *Exp. Cell Res.* 175, 84–91 (1988).

34   Reynolds SS. The use of lead citrate of high pH as an electron-opaque stain in electron microscopy. *J. Cell Biol.* 17, 208–212 (1963).

35   Lowry OH, Rosebrough NJ, Farr AL, Randall RJ. Protein measurement with the Folin phenol reagent. *J. Biol. Chem.* 193, 265–275 (1951).

36   Ribble D, Goldstein NB, Norris DA, Shellman YG. A simple technique for quantifying apoptosis in 96-well plates. *BMC Biotechnol.* 5, 12 (2005).

37   Milowska K, Szwed A, Mutrynowska M *et al.* Carbosilane dendrimers inhibit a-synuclein fibrillation and prevent cells from rotenone-induced damage. *Int. J. Pharm.* 484, 268–275 (2015).

38   Pedziwiatr-Werbicka E, Fuentes E, Dzmitruk V *et al.* Novel 'Si C' Carbosilane dendrimers as carriers for anti-HIV nucleic acids: studies on complexation and interaction with blood cells. *Colloids Surf. B Biointerfaces* 109, 183–189 (2013).

39   Koceva-Chyla A, Matczak K, Hikisz P- *et al.* Insights into the in vitro anticancer effects of diruthenium-1. *Chem. Med. Chem.* 11, 1–18 (2016).

40   Dickerson M, Sun Y, Howerton B, Glazer EC. Modifying Charge and hydrophilicity of simple Ru(II) polypyridyl complexes radically alters biological activities: old complexes, surprising new tricks. *Inorg. Chem.* 53, 10370–10377 (2014).

41   Lazniewska J, Milowska K, Katir N *et al.* Viologen-phosphorus dendrimers exhibit minor toxicity against a murine neuroblastoma cell line. *Cell. Mol. Biol. Lett.* 18, 459–478 (2013).

42   Ionov M, Ciepluch K, Garaiova Z *et al.* Dendrimers complexed with HIV-1 peptides interact with liposomes and lipid monolayers *Biochem. Biophys. Acta Biomembr.* 1848 (4), 907–915 (2015).

43   Zhao Z, Luo Z, Wu Q, Zheng W, Feng Y, Chen T. Mixed-ligand ruthenium polypyridyl complexes as apoptosis inducers in cancer cells, the cellular translocation and the important role of ROS-mediated signalling. *Dalton Trans.* 43, 17017–17028 (2014).

44   Hikisz P, Szczupak L, Koceva-Chy-   la A-   *et al.* Anticancer and antibacterial activity studies of gold(I)-alkynyl chromones. *Molecules* 20, 19699–19718 (2015).

45   Solarska-Sciuk K, Gajewska A, Gli´   nska S´   *et al.* Effect of functionalized and non-functionalized nanodiamond on the morphology and activities of antioxidant enzymes of lung epithelial cells (A549). *Chem. Biol. Int.* 222, 135–147 (2014).

46   Studzian M, Szulc A, Janaszewska A, Appelhans D, Pulaski L, Klajnert-Maculewicz B. Mechanisms of internalization ofmaltose-modified poly(propyleneimine) glycodendrimers into leukemic cell lines. *Biomacromolecules* 18, 1509–1520 (2017).

47   Tone S, Sugimoto K, Tanda K´   *et al.* Three distinct stages of apoptotic nuclear condensation revealed by time-lapse imaging, biochemical and electron microscopy analysis of cell-free apoptosis. *Exp. Cell Res.* 313, 3635–3644 (2007).

48   Chu C, Xu J, Cheng D *et al.* Anti-proliferative and apoptosis-inducing effects of camptothecin 20 (S)-O-(2-Pyrazolyl-1) acetic ester in human breast tumor MCF-7 cells. *Molecules* 19, 4941–4955 (2014).

49   Bae Y, Song SJ, Mun JY, Ko KS, Han J, Choi JS. Apoptin gene delivery by the functionalized polyamidoamine (PAMAM) dendrimer modified with ornithine induces cell death of Hepg 2 cells. *Polymers* 9, 197 (2017).